

## Scattering of 151- and 188-Mev Positive Pions by Protons\*

GEORGE HOMA, GERSON GOLDHABER,† AND LEON M. LEDERMAN  
Columbia University, New York, New York

(Received October 1, 1953)

A beam of  $\sim 200$ -Mev  $\pi^+$  mesons was defined inside the vacuum chamber of the Nevis Cyclotron. Nuclear emulsions were exposed to a flux of about  $10^4$  mesons/cm<sup>2</sup>. The plates were scanned for pion-hydrogen scatterings and 103 such events were observed in two interaction energies,  $151 \pm 7$  Mev and  $188 \pm 8$  Mev. We obtain total cross sections of  $152 \pm 31$  and  $159 \pm 34 \times 10^{-27}$  cm<sup>2</sup>, respectively. The data suggest that the angular distribution changes from backwards peaked to almost symmetric over this energy interval. Our observations are not in agreement with the hypothesis of a  $P_{1/2}$ -wave resonance in this energy region. The best fit to the combined results includes a  $D$ -wave contribution of  $-5.4^\circ$ , although satisfactory agreement may be obtained with only  $S$  and  $P$  waves.

## I. INTRODUCTION

PION-NUCLEON scattering experiments<sup>1-3</sup> have demonstrated a very strong increase of cross section with meson energy. Studies have been carried out with positive pions up to 135 Mev and negative pions up to 220 Mev.<sup>1</sup> The fruitful partial wave analyses of the angular distributions in the three possible scattering processes:  $\pi^- + p \rightarrow \pi^- + p$ ,  $\pi^- + p \rightarrow \pi^0 + n$ ,  $\pi^+ + p \rightarrow \pi^+ + p$ , have demonstrated a strong  $p$ -state interaction between pion and proton. The possibility that the coupling is strong enough to produce a resonance in the meson-nucleon interaction has recently been discussed.<sup>4</sup> The Chicago experiments do not extend far enough in energy to support this hypothesis.<sup>5</sup> This experiment was designed to yield some data on the  $\pi^+$  hydrogen scattering in the region of the suspected resonance. Positive mesons in this energy region are not conveniently studied by the techniques which have recently been employed at Columbia and Chicago.

These have made use of external meson beams. The focusing action of the cyclotron fringing field is effective only for negative mesons which are produced roughly in the forward direction, and positive mesons produced in the backward direction with respect to the proton beam. The velocity of the center of mass in the production process results in a large decrease in the yield of high-energy positive mesons. At Nevis, external  $\pi^-$  beams up to 160 Mev are obtained with good flux, whereas the highest usable  $\pi^+$  beam reaches 85 Mev. In this experiment, use was made of the forward-produced positive mesons which are deflected into the cyclotron from the target. Photographic emulsions were used to detect these particles. The technique of using the hydrogen content of the emulsion as the scatterer had already been used with external beams<sup>6</sup> and was employed here.

## II. EXPERIMENTAL PROCEDURE

Positive pions produced by the 385-Mev proton beam in a beryllium target are focused at  $180^\circ$  by the cyclotron magnet. In the energy region of interest, 150–200 Mev, the focusing point is about one-third the distance from the cyclotron center along a radius to the target (see Figs. 1 and 2). The dispersion in this region is about 6 Mev per inch of radial displacement. The problem was to obtain good exposures of Ilford G-5 emulsions to these high-energy mesons, with minimum

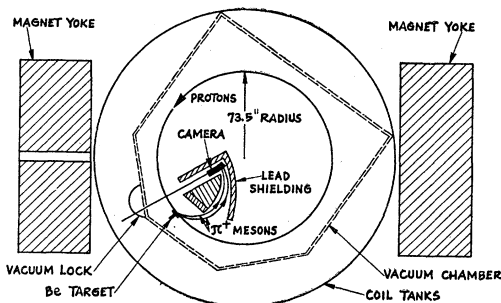


FIG. 1. Plan view of internal exposure.

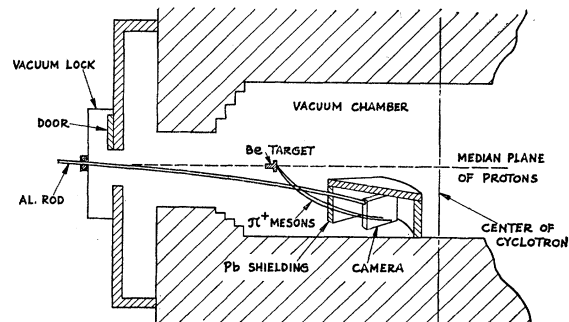


FIG. 2. Elevation view of internal exposure.

\* This research was supported by the joint program of the U. S. Office of Naval Research and the U. S. Atomic Energy Commission.

† Now at the Physics Department, University of California, Berkeley, California.

<sup>1</sup> Anderson, Fermi, Martin, and Nagle, Phys. Rev. **91**, 155 (1953).

<sup>2</sup> Bodansky, Sachs, and Steinberger, Phys. Rev. **90**, 996 (1953).

<sup>3</sup> J. P. Perry and C. E. Angell, Phys. Rev. **91**, 1289 (1953).

<sup>4</sup> K. A. Brueckner, Phys. Rev. **86**, 106 (1952).

<sup>5</sup> Martin, Fermi, and Nagle [Phys. Rev. **91**, 467 (1953)] have recently reported results for 169- and 192-Mev  $\pi^-$  scattering.

<sup>6</sup> G. Goldhaber, Phys. Rev. **89**, 1187 (1953).

TABLE I. Typical energy evaluation from proton range calibration.

Proton Steps	$R_p^a$ $\mu$	$R_p(\text{Cu})^b$ $\text{g/cm}^2$	$T(\text{Cu})^c$ $\text{g/cm}^2$	$E_p^d$ Mev	$E_\pi^e$ Mev
1	7700	3.06	0.64	$52.1 \pm 1$	$205.7 \pm 3$
2	5900	2.31	1.49	$52.8 \pm 1$	$207.7 \pm 3$
3	4700	1.83	1.92	$52.5 \pm 1$	$206.8 \pm 3$
4	3400	1.32	2.35	$51.9 \pm 1$	$205.2 \pm 3$
5	2400	0.935	2.78	$52.2 \pm 1$	$206.0 \pm 3$

Result:  $206 \pm 1$  Mev. Result from position in magnetic field:  $208 \pm 3$  Mev.

<sup>a</sup> Residual range of protons in emulsion,  $R_p$  (see Fig. 4).

<sup>b</sup> Equivalent range in Cu,  $R_p(\text{Cu})$ .

<sup>c</sup> Thickness of Cu absorber steps on camera cover  $T(\text{Cu})$ .

<sup>d</sup> Proton energy incident on camera  $E_p$ .

<sup>e</sup> Meson energy incident on camera (of same momentum)  $E_\pi$ . The mesons incident on the emulsions have to penetrate the camera cover 0.2 in. of Cu and their energy is thus reduced by  $\approx 7$  Mev.

background, and to scan these plates for  $\pi^+$ -H scattering events. The exposures were carried out in a vacuum-tight camera which was introduced into the cyclotron chamber through a vacuum lock at the end of a long rod. In this manner the emulsions were kept at normal pressure and humidity conditions during the exposure.

The camera, in its final position, rested upon the lower cyclotron pole face, the plane of the emulsions vertical and the long edge facing the meson beam. The camera was mounted in a 2-in. thick brass block which provided extra shielding and which adjusted the tilt of the emulsion so as to receive the beam perpendicular to the long edge. The assembly was pushed into a predetermined position within a mass of lead-shielding bricks which were strategically disposed on the magnet face. Two curved channels defined the meson trajectories; one at 165 Mev and one at 205 Mev. In spite of about 1 ton of lead shielding, it was discovered that to avoid blackening the plates the exposures had to be of the order of 3-5 seconds. After a particular shielding arrangement had been installed, it was found that continuous operation of the cyclotron for several hours would produce radioactivity in the lead bricks. This added serious background in the 10-20 minutes during which the camera was being pushed in and out of the vacuum chamber. Exposures were therefore carried out only after a shutdown of the cyclotron for several days and with a fresh "inner lining" of lead bricks. In this way, plates were obtained having track densities of  $\sim 10^4$  mesons/cm<sup>2</sup> with acceptable background. Ilford G-5 600 $\mu$  and 400 $\mu$  plates were used.

### III. ENERGY CALIBRATION

The scattering cross sections are known to vary greatly with energy of the meson. This made necessary a rather precise determination of the interaction energy. Three independent methods were employed to this end.

(1) The location of the emulsions relative to the proton target in the magnetic field of the cyclotron was used to compute the momentum of the particles incident upon the camera. The exposures resulted in a quite parallel flux of particles in the proper direction. Thus no

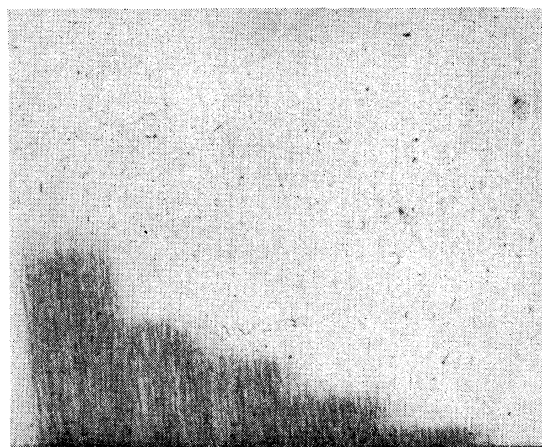


FIG. 3. Proton range curve in nuclear emulsion exposed to 318-Mev/c particles. The longest step is actually 8 mm in length. The steps correspond to increasing thicknesses of brass absorber.

important contribution could be made by mesons either scattering in the collimator or originating outside of the target. The average value of the cyclotron field over the trajectory was 17 300 gauss. Particles traversing the higher-energy channel had a maximum momentum of 318 Mev/c. This corresponds to a pion kinetic energy of 208 Mev. Ten plates were exposed simultaneously across the 2.5-in. channel breadth. The energy interval over the high-energy channel was 2.5 in.  $\times 6$  Mev/inch = 15 Mev. Similarly, the low-energy channel was centered about 165 Mev.

(2) The selected momentum of 318 Mev/c corresponds to a proton energy of 52 Mev. Protons of this energy are made far more copiously than the mesons and had to be prevented from reaching the emulsion. A 0.20-in. brass cover plate was used to stop the protons. A series of five grooves were milled in the lower half-inch of the cover plate in order to obtain a range curve of the incident protons. Where the grooves were deep enough, the heavily ionizing protons were able to reach and blacken the emulsion. Correspondingly, each nuclear track plate then had a series of steps indicating the residual range of the protons incident upon it. This range was converted to proton momentum incident upon the cover plate. The energy of the pions was obtained by assuming them to have the same momentum as the protons. Figure 3 is an enlargement of a nuclear emulsion exposed to  $318 \pm 5$  Mev/c particles. The parallelism and monochromaticity of the protons is additional evidence in favor of the validity of the geometry. Table I presents an analysis of the proton range curve in a typical plate. The results obtained by this method are in excellent agreement with the energy as determined from position in the magnetic field.

The incident meson energy is reduced by its ionization loss in the 0.20-in. brass cover plate and by one-half the loss in traversing the emulsion (average lengths

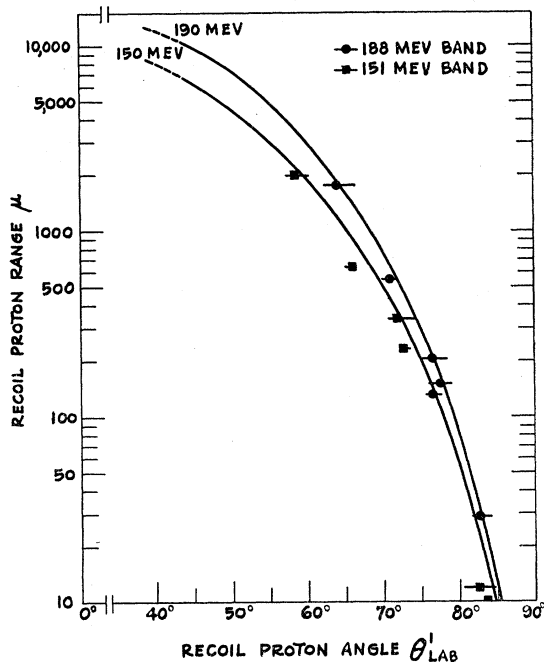


FIG. 4. Range-angle correlation for recoil protons in  $\pi^+p$  collisions.

were  $4000\mu$ ). The resulting interaction energies were  $151 \pm 7$  Mev for the low-energy exposure,  $188 \pm 8$  Mev for the high-energy exposure.

(3) In the  $\pi^+$  hydrogen collisions, it occasionally happened that the recoil proton stopped in the emulsion. This was used to recalculate the meson energy. The results are given in Fig. 4 where the observed cases are plotted on a curve of proton range *vs* proton recoil angle.

The proton recoil angles plotted are the "best fit" values of the experimental  $\theta$  and  $\varphi$  measurements to the angular correlation curve (Fig. 6), where  $\theta$  and  $\varphi$  are the proton recoil and meson scattering angles, respectively. The extremities of the angular uncertainty shown in Fig. 4 correspond to the measured values of  $\theta$  and  $\varphi$ . As can be seen from the curves, the energy determinations are extremely sensitive to errors in proton recoil angle. The present method can only be considered as a confirmation of the previously described techniques.

#### IV. SCANNING PROCEDURE

The presence of a comparatively large background of proton tracks ruled out the possibility of employing area scanning with any assurance of good scanning efficiency. Instead, the far more laborious method of track scanning was adopted. In this technique, the scanner selects a track satisfying ionization and directional criteria and follows it under  $10 \times 45$  (oil) or  $10 \times 90$  (oil) magnification until it either leaves the plate or interacts. Essentially 100 percent efficiency for the detection of all types of events should be obtained with this method. All scatterings through angles greater

than  $1^\circ$  were recorded. Figure 5 gives the frequency per meter of track in projected angle intervals less than  $30^\circ$ . These results were used to obtain good statistics on relative efficiency among the various scanners. To the extent that nuclear effects are small below  $15^\circ$ , this also constitutes a comparison with a known (Rutherford) cross section and an order of magnitude check on the over-all scanning efficiency. The agreement with Coulomb scattering begins above  $7^\circ$ . However, hydrogen collisions are associated with heavily ionizing recoil proton tracks and are much more prominent than small angle elastic scatterings.

The observed events were categorized as stops in flight, elastic scatterings, one-prong ("inelastic") scatterings, one-prong stars and stars of two to nine prongs. The one-prong events were all considered as possible hydrogen events and subjected to the detailed measurements described below. An additional measure of relative efficiency compared the ratio of all types of meson interactions resulting in one black prong to observed path length and to the number of stars with two or more prongs. These comparisons, together with the elastic scattering data, led to the conclusion that the track scanning, especially on plates of high background, were not necessarily 100 percent efficient. We

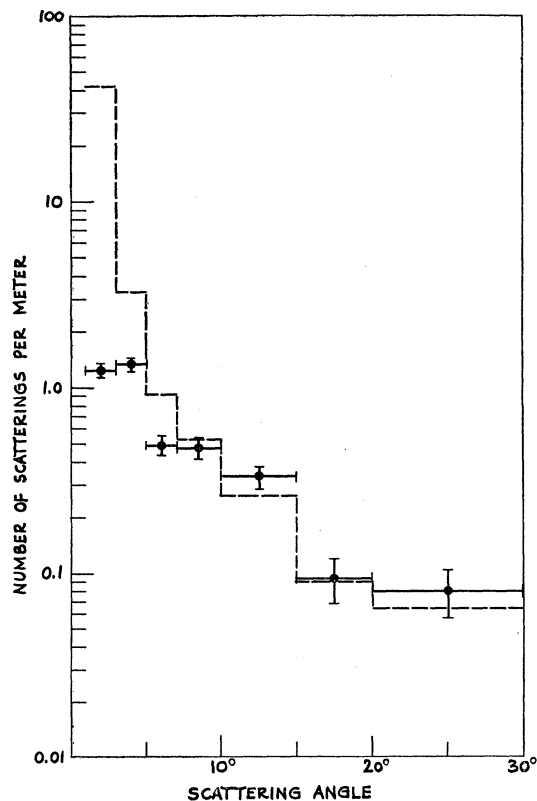


FIG. 5. Elastic scatterings of high-energy pions in nuclear emulsion. Projected angles of scattering are given. The dashed curve is the projected angular distribution due to Rutherford scattering averaged over the emulsion contents.

estimated that an over-all variation of 12 percent existed in the efficiency for finding one-prong events. Since this is always a negative effect, a correction of half this amount was made to the data and the uncertainty in the scanning efficiency was taken as  $\pm 10$  percent.

### V. THE IDENTIFICATION OF $\pi^+ + H$ SCATTERING EVENTS

Because of energy and momentum conservation in the  $\pi^+ + H$  scattering interaction, such events can be identified on the basis of the two criteria:

1. Coplanarity of the three prongs  $\pi$ ,  $\pi'$ , and  $p$ .
2. Angular correlation between the scattered meson ( $\pi'$ ) and the recoil proton ( $p$ ).

An additional confirmation is obtained from the range-angle correlation for those recoil protons which end in the emulsions (Fig. 4). All events with one proton prong found in the course of the scanning were carefully examined for possible associated scattered mesons. These events with one proton and a scattered meson were measured. Measurements were made of the two projected angles (in the plane of the emulsion)  $\alpha_{\pi'}$  and  $\alpha_p$ , the three dip angles  $\beta_{\pi}$ ,  $\beta_{\pi'}$ , and  $\beta_p$ , and the range of the recoil proton  $R_p$ .

The details of the analysis are presented in Figs. 6, 7, and 8 for those events found in 173 meters of track scanning. The quantity  $F = \tan\beta_{\pi'} \sin\alpha_p - \tan\beta_p \sin\alpha_{\pi'} - \tan\beta_{\pi} \sin(\alpha_{\pi'} - \alpha_p)$  is proportional to the volume of a pyramid formed by the center of the event and 3 points unit distance along each of the 3 vectors  $\pi$ ,  $\pi'$ ,

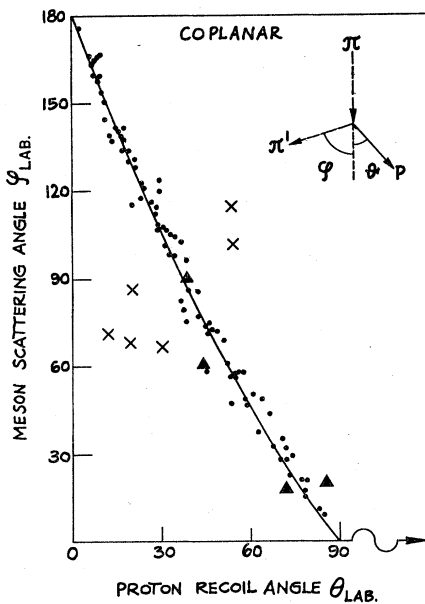


Fig. 6. Angular correlation relating the meson scattering angle and the proton recoil angle. The triangles represent "doubtful" cases. The crosses represent events which satisfied coplanarity requirements but are excluded because of lack of correlation. The dots represent  $\pi$ - $p$  collisions.

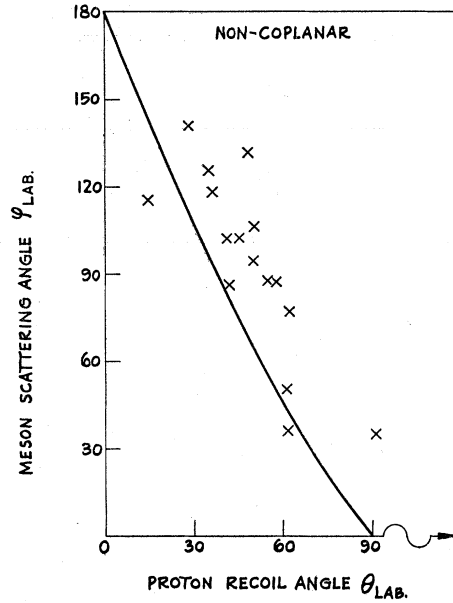


Fig. 7. Distribution of noncoplanar events about the angular correlation curve. Events having a proton emitted backwards are not included.

and  $p$ .  $F$  was computed for all events as a measure of the coplanarity where  $F \rightarrow 0$  corresponds to coplanarity. Figures 6 and 7 give the angular correlation curves between meson scattering angle  $\varphi_{\text{lab}}$  and proton recoil angle  $\theta_{\text{lab}}$  which follow from the kinematics of  $\pi$ - $P$  scattering. All events with  $F/\Delta F \leq 2.5$  are called "coplanar" and are given in Fig. 6, where  $\Delta F$  is the rms error in  $F$  based on the various individual measuring errors. All other events are called "noncoplanar" and for clarity are given separately in Fig. 7. In Fig. 8 we plot  $F/\Delta F$  vs  $\Theta/\Delta\Theta$  where  $\Theta = (\delta\theta^2 + \delta\varphi^2)^{1/2}$  is the deviation from the angular correlation curve (Figs. 6 and 7) and  $\Delta\Theta$  is again the rms error due to measurements.

Of the 104 events on Fig. 8, 75 events lie in the circle of radius 1.75 in units of the rms measuring errors, 4 events lie between the radii 1.75, and 2.5 and 25 events lie outside the radius 2.5. These events are classified as "sure"  $\pi + p$  events, "doubtful"  $\pi + p$  events and "not"  $\pi + p$  events, respectively, and are represented by different symbols in Figs. 6, 7, and 8.

An additional check on the identification of hydrogen scatterings was made by grain-counting all scattered mesons of sufficient length ( $> 400\mu$ ). The ratio of grain densities of the incident and scattered meson is related to the angle of scattering. At these energies, this is not a sensitive test unless the tracks are very long. One event, satisfying all other criteria, was discarded by this test. All other measurable cases were consistent

<sup>7</sup> Figures 6, 7, and 8 do not include events in which the proton goes in the backward direction ( $\alpha_p > 90^\circ$ ) or events in which the projection on the plane of the emulsion of  $\pi'$  and  $p$  are both on the same side of  $\pi$  (i.e., the signs of  $\alpha_{\pi'}$  and  $\alpha_p$  are equal). Such events can be excluded on visual inspection from being possible  $\pi$ - $p$  scattering events.

TABLE II. Evaluation of total cross section.

Energy Mev	Total path (meters)	Path corrected for 10±10% $\mu+e$	No. of nuclear interactions	Path obtained from $\lambda=31.7$ cm	No. of $\pi+p$ obs. events	No. of events corrected	Cross section $\times 10^{-27}$ cm <sup>2</sup>
151±7	95.34	85±8.5	260	82.5±9.0	41	43	152±31
188±8	77.44	70±7.0	225	71.0±8.0	34	38	159±34
Combined 168	172.78	155±16	485	153.5±17	75	81	155±24

with the identification as  $\pi+p$  scatterings. The “not”  $\pi+p$  events are inelastic scatterings from other nuclei in the emulsion, in which one proton is emitted, possibly accompanied by one or more neutrons. The meson momentum of about 300 Mev/c is comparable to the Fermi momentum of the nucleons. Quasi-elastic<sup>8,9</sup> collisions can thus take place. These should have a very broad distribution around the  $\pi+p$  correlation curve. A background density of these events may be obtained from Fig. 8. The contribution of this density to the cross section was computed to be 1 to 2 events. It is interesting to note that in previous work<sup>6</sup> at  $E_\pi=75$  Mev ( $P_\pi=165$  Mev/c, which would give an even broader distribution) no evidence was seen for quasi-elastic scattering. (At that energy the  $\pi^++p$  cross section is also considerably smaller.) Similarly, with negative pions at  $E_\pi=135$  Mev,<sup>10</sup> no evidence for quasi-elastic scattering was seen in emulsions. Here again the  $\pi^-+p$  cross section is much smaller and presumably  $\pi^-+“N”$  quasi-elastic scattering occurs.

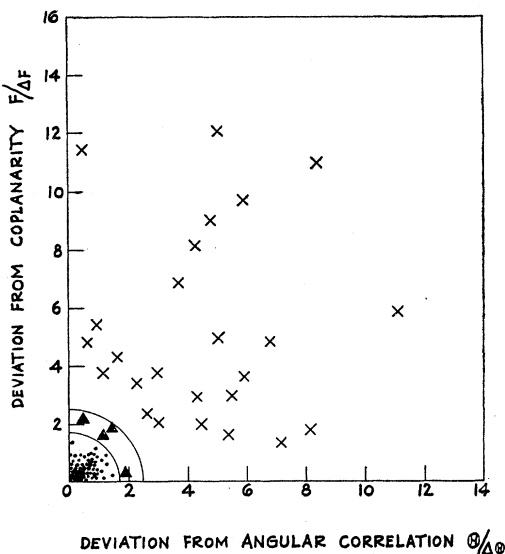


FIG. 8. Distribution of one-prong events in correlation space. The dots represent “sure” hydrogen collisions. The triangles represent doubtful cases. The crosses represent background. Only events which were observed in the 173 meters of track scanning are included here.

<sup>8</sup> Cladis, Hess, and Moyer, Phys. Rev. **87**, 425 (1952).

<sup>9</sup> P. A. Wolff, Phys. Rev. **87**, 434 (1952).

<sup>10</sup> G. Goldhaber and S. Goldhaber, Phys. Rev. **91**, 467 (1953).

## VI. ANALYSIS OF DATA

### A. Total Cross Sections

A total of 173 meters of track was recorded for the determination of the total cross sections. We have observed 535 nuclear interactions of all kinds, including 75 which were classified as certain hydrogen events. See Table II.

External meson beams are known to contain contaminations of muons and electrons. The electrons are very probably made in the cyclotron target by conversion of  $\pi^0$   $\gamma$  rays. The insensitivity of the mu “tail” in range curves to geometry<sup>11</sup> is evidence that most of the muons originate near the target. Thus it seems reasonable to assume that similar contaminations are present in internal fluxes.<sup>12</sup> Using the data on mu and electron contaminations in the external  $\pi^-$  (forward-produced) beams we have estimated that the internal flux is  $90 \pm 10$  percent pions.

An independent evaluation of the pion flux is made by considering the total reaction cross section (stars, stops, inelastic scattering) observed in these plates and recalling that muons and electrons do not contribute significantly to these processes.<sup>13</sup> The total interaction of 135- and 210-Mev negative pions in emulsions has recently been observed with similar (along the track) scanning methods.<sup>10,14</sup> In addition, it is known that above 100 Mev, the total cross section is quite insensitive to meson energy.<sup>15</sup> To compare the data obtained here with the approximately known fluxes of negative pions, one must take into account Coulomb effects. The Coulomb field can modify the reaction cross section according to the classical relation:<sup>16</sup>

$$\frac{\sigma(+)}{\sigma(-)} = \frac{1 - V(R)/E}{1 + V(R)/E},$$

where  $E$  is the kinetic energy and  $V(R)$  is the Coulomb barrier at the surface of the nucleus. This effect has

<sup>11</sup> H. Loar and R. Durbin (private communication).

<sup>12</sup> Although the electron contamination decreases strongly with increasing energy of the meson beam, a 4-percent contamination has been observed in the 135-Mev  $\pi^-$  beam by means of a cloud chamber containing thin lead plates.

<sup>13</sup> A total of 8 stops in flight were observed. If these are all due to positron annihilation, this would be consistent with a 3 percent contamination.

<sup>14</sup> A. H. Morrish, Phys. Rev. **90**, 674 (1953).

<sup>15</sup> R. L. Martin, Phys. Rev. **87**, 1052 (1952); Chedester, Isaacs, Sachs, and Steinberger, Phys. Rev. **81**, 918 (1951).

<sup>16</sup> J. M. Blatt and V. F. Weisskopf, *Theoretical Nuclear Physics* (John Wiley and Sons, Inc., New York, 1952), p. 346.

TABLE III. Differential cross sections of  $\pi^+$  mesons on protons ( $10^{-27}$  cm<sup>2</sup>/sterad).<sup>a</sup>

Lab. energy Mev	Cm. Angular interval					
	8-30°	30-60°	60-90°	90-120°	120-150°	150-180°
151±7	10.3±4.2	8.3±2.3	8.7±2.5	6.1±1.6	20 ±3.2	39±8
188±8	21.5±6.5	9.0±2.6	9.8±2.2	12 ±2.7	14.8±3.5	24±7
168±30	15.2±3.5	8.5±1.6	9.1±2.0	8.6±1.4	17.6±2.2	32±5.1

<sup>a</sup> The errors shown are probable errors arising from statistics only.

been observed in a direct comparison of  $\pi^+$  and  $\pi^-$  meson reactions at 60 Mev and at 110 Mev.<sup>17</sup> For emulsions at 170 Mev this is a 10-percent effect. Accordingly, the mean free path for all nonelastic processes of references 10 and 13 was increased by 10 percent. This gave a result of  $31.7 \pm 3.3$  cm of emulsion. The total number of nuclear events observed in this experiment included 75 hydrogen scatterings, whereas the hydrogen contribution to the  $\pi^-$  experiments was only of the order of  $\frac{1}{3}$  as much.<sup>1</sup> Thus we used 485 events (Table II) to make the comparison.<sup>18</sup> The flux obtained by this method is then  $485 \times 0.317 = 153.5$  meters. This is in (fortuitously) excellent agreement with the estimate of 10-percent beam contamination. Table II contains a breakdown in the two energy intervals. The corrections to the observed number of hydrogen events include a subtraction due to background (Sec. V, 2 events), and an addition (6 events) due to scanning efficiency (Sec. IV). In the evaluation of the error, we have included the statistical standard deviation, and the contributions to possible systematic errors from the flux, scanning efficiency, doubtful and background events, and the small uncertainty in the density of hydrogen in the emulsion.<sup>19</sup>

### B. Angular Distribution

There were 103 events acceptable for the angular distribution. Some of these were found by area scanning in the vicinity of selected meson tracks. Most of these were found in track scanning outside of the prescribed region in which the total path length was counted.

For meson scattering angles greater than  $5^\circ$  the range of the recoil proton is greater than  $10\mu$ . Thus essentially no bias can be introduced into the angular distribution by the various methods of detection. The results are plotted in Fig. 9 and listed in Table III. We also include the results of averaging the two energy intervals. The errors shown are only the probable errors arising from statistics and do not include the normalization un-

certainty. Systematic errors here would presumably be due only to the inclusion of background events (quasi-elastic scatterings) which have the same kinematics as free  $\pi+P$  collision. Recent data obtained at lower energies (135 Mev) on inelastic scattering in C, Pb,<sup>20</sup> and emulsion<sup>10</sup> indicate that this background would, if present in any significant proportion, increase the ratio of backward to forward scattering. A cutoff at small angles is forced by the range of recoil protons. We have set  $10\mu$  as the minimum acceptable range. This corresponds to a meson scattering angle of  $5^\circ$  in the laboratory system and  $8^\circ$  in the cm system. Coulomb contributions are expected to be negligible above  $15^\circ$  although interference effects may be contributing to the 8-30° interval. These probably act to depress this point slightly.<sup>2</sup>

### VII. DISCUSSION

Figure 10 summarizes recent determinations of the  $\pi^+$  total cross section as a function of meson energy. Data are included from Chicago,<sup>1</sup> Columbia,<sup>2</sup> Rochester,<sup>3</sup> and from a diffusion cloud chamber study at Brookhaven.<sup>21,22</sup> One of the most interesting questions raised by these data is that of the detection of nucleon structure. A feature of strong-coupling pseudoscalar meson theory is the existence of isobaric levels having definite angular momentum and isotopic spin assignments. The specific level presumed to be responsible for the scattering at these energies is the  $J = \frac{3}{2}, I = \frac{3}{2}$  level. The phenomenological introduction of such a

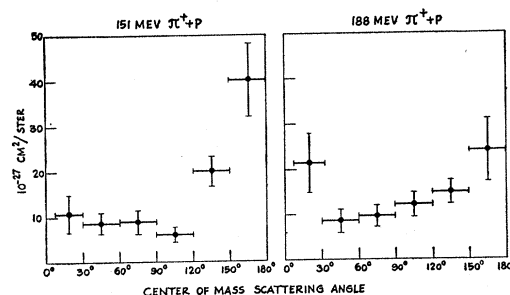


Fig. 9. Differential cross sections of 151- and 188-Mev pions in hydrogen. The uncertainties are the probable errors due to statistics only.

<sup>20</sup> J. Kessler and L. M. Lederman (to be published).

<sup>21</sup> Fowler, Lea, Shephard, Shutt, Thorndike, and Wittemore, Phys. Rev. **92**, 832 (1953).

<sup>22</sup> S. Lindenbaum and L. C. L. Yuan have recently obtained a value of 48 mb at 340 Mev. This confirms the decrease at higher energies suggested by Fig. 10.

<sup>17</sup> Byfield, Kessler, and Lederman, Phys. Rev. **86**, 17 (1952); Aarons, Ashkin, Feiner, Gorman, and Smith, Phys. Rev. **90**, 342 (1953).

<sup>18</sup> The weakness of this method lies in the uncertain efficiency of the  $\pi^-$  scanning for the detection of very small events, principally stops-in-flight. These are either absorptions with neutron emission or charge exchange scatterings. In both cases, the corresponding events with positive mesons are associated with heavily ionizing prongs and are more easily detected. Stops constitute about 10 percent of the reaction cross section in the  $\pi^-$  work.

<sup>19</sup> Goldhaber, Biell, Frankl, and Goldhaber, Rev. Sci. Instr. (to be published).

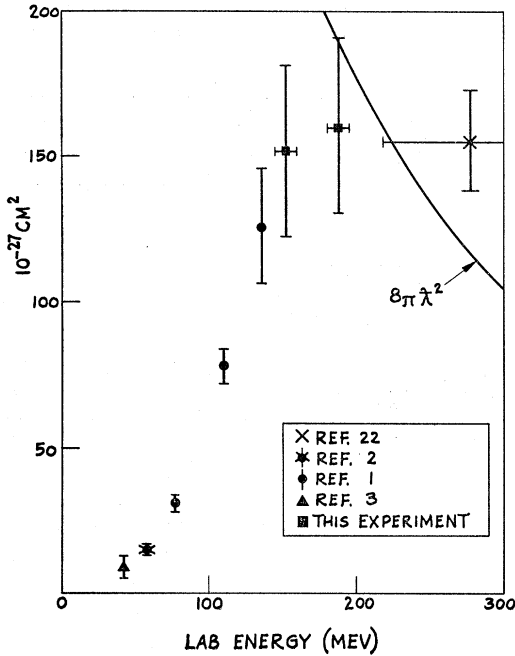


FIG. 10. Variation of total cross section of  $\pi^+$  mesons with energy. Recent results from Brookhaven [S. Lindenbaum and L. Yuan (private communication)] indicate a cross section of  $48 \pm 9$  mb at 340 Mev.

resonance at  $E \sim 200$  Mev has been successful in fitting the lower-energy pion-nucleon scattering<sup>4</sup> and the photomeson production data.<sup>23</sup> In addition, recent results<sup>24</sup> at higher photon energies have shown a very rapid decrease in cross section above 320 Mev, again suggesting a resonance in the meson-nucleon interaction.

The most direct evidence for the resonance must come from the  $\pi^+$  scattering data since only this experiment involves a pure  $I = \frac{3}{2}$  state. Although Fig. 10 clearly shows the provisional nature of the results in the resonance region, the present experiment tends not to support the resonance hypothesis. To demonstrate this, a phase shift analysis has been made. Following Anderson *et al.*<sup>1</sup> we assumed only  $S$  and  $P$  waves, and so fitted the data with a distribution of the form

TABLE IV. Least-squares fit of the data to the form  $d\sigma/d\Omega = a + b \cos\theta + c \cos^2\theta \times 10^{-27}$  cm<sup>2</sup>/sterad.

Lab. energy Mev	$a$	$b$	$c$
78 <sup>a</sup>	$1.9 \pm 0.3$	$-1.7 \pm 0.4$	$1.6 \pm 0.9$
110 <sup>a</sup>	$3.6 \pm 0.7$	$-4.8 \pm 0.8$	$7.5 \pm 1.9$
135 <sup>a</sup>	$3.9 \pm 2.3$	$-7.1 \pm 2.8$	$18 \pm 6.8$
151	$6.2 \pm 2.4$	$-7.7 \pm 2.6$	$19 \pm 5.0$
188	$10 \pm 3.5$	$-4.1 \pm 2.0$	$8.7 \pm 2.8$
Combined $E = 168$	$7.7 \pm 2.0$	$-6.1 \pm 2.1$	$14.6 \pm 3.2$

<sup>a</sup> See reference 1.

<sup>23</sup> K. A. Brueckner and K. M. Watson, Phys. Rev. **86**, 923 (1952).

<sup>24</sup> Walker, Oakley, and Tollestrup, Phys. Rev. **89**, 1301 (1953).

$a + b \cos\theta + c \cos^2\theta$ . This is given in Table IV. The result of combining the data for the two energy intervals is also given. The equations relating the three phase shifts,  $\alpha_3$ ,  $\alpha_{33}$ , and  $\alpha_{31}$ ,<sup>25</sup> to the three parameters  $a$ ,  $b$ , and  $c$  are transcendental. Graphical<sup>26</sup> and numerical investigations of these equations show that there exist sets of  $a$ ,  $b$ ,  $c$ 's for which solutions do not exist. Angular distributions which yield such sets are presumably inconsistent with the assumption of only  $S$  and  $P$  wave contributions to the scattering. In the present experiment, the distributions given in Table IV fall in this category. However, the errors are large and it is always possible to obtain solutions by varying the  $a$ ,  $b$ , and  $c$  coefficients within the experimental uncertainties. The results of such variations corresponding to the Fermi-type solutions<sup>1</sup> are given in Table V. The least squares sum,

$$M = \sum_i^6 \left( \frac{\delta_i}{PE_i} \right)^2,$$

where  $\delta_i$  are the deviations of the phase-shift results from the observed points and  $PE_i$  are the probable errors, is also given. In each case, an attempt, by no means exhaustive, was made to minimize  $M$ . Large but difficult to compute uncertainties go with these phase shifts.

We have investigated the effect on the  $\alpha$ 's of a small  $D$ -wave contribution. It has been theoretically noted<sup>27</sup> that  $D$ -wave scattering should accompany the large  $P$  scattering as a nucleon recoil effect. Choosing the largest  $D$  phase shift,<sup>27</sup> the  $D_{\frac{3}{2}}$ ,<sup>3</sup> and keeping only interference terms (we assume  $\alpha_{31}$  small here), results in a  $\cos^2\theta$  term with coefficient  $12\lambda^2 \sin\alpha_{33} \sin d_{53} \cos(d_{53} - \alpha_{33})$ . The data very much require this term and hence  $d_{53}$  to be negative with respect to  $\alpha_{33}$ , in agreement with theory. One such solution for  $E = 168$  Mev (combined data) is given in Table V. It is interesting to note that the  $\alpha_3$  phase shift has been strongly decreased by the  $-5.4^\circ$  of  $D$  wave. All of the distributions in Table V "fit" the observations. However, the fact that the actual experimental values at 168 Mev seem to require  $D$  waves (not outside of experimental errors) raises the question of the existence of any *a priori* theoretical prejudice against this conclusion. On the other hand, a reinterpretation of the lower energy data on the basis of a small negative  $D$  wave could lead to a simpler  $S$ -wave energy dependence.

Table V shows that the  $\alpha_{33}$  phase shift is of the order of  $40$ – $55^\circ$  over this energy interval. Thus, at least up to 190 Mev, no evidence for a resonance is observed. To re-enforce this conclusion we note that for a resonant interaction in the  $P_{\frac{3}{2}}$  state, the total cross section would have to be at least  $8\pi\lambda^2$ . This is just inside of the

<sup>25</sup> We use the notation of reference 1.

<sup>26</sup> J. Ashkin and S. H. Vosko, Phys. Rev. **91**, 1248 (1953).

<sup>27</sup> E. M. Henley and M. Ruderman, Phys. Rev. **90**, 719 (1953).

experimental errors. However, any additional states contributing to the scattering would add to the total cross section. The angular distributions are qualitatively different from a pure  $P_{\frac{3}{2}}$  state ( $1+3\cos^2\theta$ ). In fact, if one assumes  $\alpha_{33}$  near  $90^\circ$ , then, independent of any normalization, the angular distribution at 188 Mev would imply an even-wave contribution of at least 40 mb.<sup>28</sup> Thus the total cross section would have to be larger than 240 mb. No such argument may be made against a possible  $\alpha_{31}$  resonance. The experimental momentum dependence of the  $\alpha_{33}$  phase shift suggests a leveling-off although an extrapolation to  $90^\circ$  at about 230 Mev is possible.

<sup>28</sup> This is obtained by forming the ratio  $[\sigma(0^\circ)+\sigma(180^\circ)]/2[\sigma(90^\circ)]$  as  $\alpha_{33}\rightarrow 90^\circ$ . For the 188-Mev case, this is  $2.1\pm 1.0$  and implies  $\sin^2\alpha_3 > 0.5$  or  $\sigma_T > 2.5(4\pi\lambda^2)$ .

TABLE V. Phase-shift solutions.

Lab. energy Mev	Phase shifts	M
151	$\alpha_3 = -30^\circ, \alpha_{31} = 8^\circ, \alpha_{33} = 45^\circ$	12
188	$\alpha_3 = -35^\circ, \alpha_{31} = +0^\circ, \alpha_{33} = 55^\circ$	15
Combined $\bar{E}=168$	$\alpha_3 = -40^\circ, \alpha_{31} = 12^\circ, \alpha_{33} = 40^\circ$	10
$\bar{E}=168$ and D waves	$\alpha_3 = -23^\circ, \alpha_{31} = -8^\circ, \alpha_{33} = 50^\circ$ $d_{33} = -5.4^\circ$	4.5

The authors wish to acknowledge the contribution of the scanners, B. Kuharetz, M. Johnson, M. Hecht, and R. Klein, to this work. D. C. Peaslee's computation group assisted greatly in the analysis of the track measurements.

## Neutron Production by Cosmic Rays\*

WILLIAM C. G. ORTEL†

*Sloane Physics Laboratory, Yale University, New Haven, Connecticut*

(Received September 9, 1953; revised manuscript received November 4, 1953)

An experimental study has been made of the production of neutrons in the nuclear interactions of cosmic rays. An apparatus selected events in which a nuclear interaction occurred in or near a liquid scintillation counter, with the production not only of ionizing particles but also of neutrons of a few Mev energy which were slowed to thermal energy in a paraffin moderator and detected by  $\text{BF}_3$ -filled proportional counters. Such coincidences are termed  $(s,n)$ ,  $(s,2n)$ , and so on, according to the number of detected neutrons. The average number,  $\bar{\nu}$ , of neutrons produced per disintegration was calculated from the observed relative numbers of  $(s,n)$  and  $(s,2n)$  coincidences.

These data were obtained at Climax, Colorado, at an altitude of 11 200 ft. Analysis shows that events of the type selected in this experiment account for the production of  $3\times 10^{-4}$  neutrons  $\text{g}^{-1}\text{sec}^{-1}$ , a figure which is close to the total neutron-production rate in carbon as previously measured at the same location. In these events, it is concluded that  $\bar{\nu}=1.3\pm 0.2$ . Combination of this result with previously determined relative multiplicities yields the values  $\bar{\nu}=2.2$  for production in aluminum and  $\bar{\nu}=6$  for production in lead.

### I. INTRODUCTION

EVIDENCE that neutrons are produced by cosmic rays in their interactions with matter was sought and found soon after the discovery of the neutron.<sup>1</sup> It is believed that the predominant neutron-production process must be the type of high-energy nuclear disintegration observed as a "star" in nuclear emulsion. The ionizing particles produced in stars are accessible to study since they leave tracks, or "prongs," in emulsion.

\* This paper is an adaptation of a dissertation presented to the Graduate School of Yale University in candidacy for the degree of Doctor of Philosophy. The work was supported in part by the joint program of the U. S. Office of Naval Research and the U. S. Atomic Energy Commission. Preliminary results were presented at the Cambridge meeting of the American Physical Society in January, 1953.

† U. S. Atomic Energy Commission Predoctoral Fellow.

<sup>1</sup> G. L. Locher, *Phys. Rev.* **44**, 779 (1933) and J. Franklin *Inst.* **224**, 555 (1937); L. H. Rumbaugh and G. L. Locher, *Phys. Rev.* **49**, 855 (1936); E. Schopper, *Naturwiss.* **25**, 557 (1937); E. M. Schopper and E. Schopper, *Physik. Z.* **40**, 22 (1939); E. Fünfer, *Naturwiss.* **25**, 235 (1937) and *Z. Physik* **111**, 351 (1938).

It has been established<sup>2</sup> that in emulsion exposed at mountain altitude the mean number of prongs per star of one or more prongs is 2.2 and that many prongs represent protons of energy near 10 Mev. It is reasonable that neutrons of comparable energy and number should also be produced. Direct measurement of these neutrons is severely restricted by the low efficiency of all available neutron detectors, and the mean number, or "multiplicity," of neutrons produced in one act has remained quite uncertain.

A number of comparisons of the over-all rates of neutron and star production have been made. All these involve two extrapolations. First, some adjustment must be made to allow for the difference in the materials for which the neutron and star rates have been measured. Second, the star rate must be corrected for the disintegrations involving 2, 1, and 0 ionizing secondaries, which are events difficult or impossible to observe

<sup>2</sup> P. E. Hodgson, *Phil. Mag.* **42**, 82 (1951); N. C. Barford and G. Davis, *Proc. Roy. Soc. (London)* **A214**, 225 (1952).



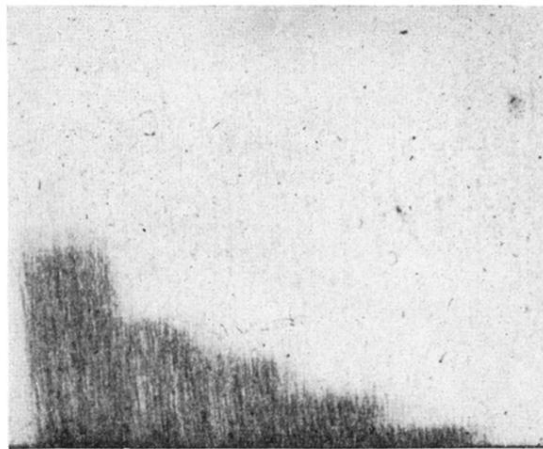


FIG. 3. Proton range curve in nuclear emulsion exposed to 318-Mev/c particles. The longest step is actually 8 mm in length. The steps correspond to increasing thicknesses of brass absorber.